sciendo Applied Mathematics and Nonlinear Sciences, 9(1) (2024) 1-13

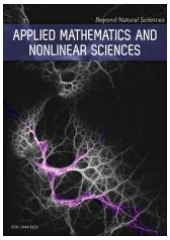

Applied Mathematics and Nonlinear Sciences

https://www.sciendo.com

Color design of modern architectural interior space based on environmental psychology

Wei Feng[1], Dan Gao[1], Yacong Guo[1], Yu Gu[1,†]

1. Department of Environmental Design, School of Architecture and design, Hebei Institute of Engineering and Technology, Shijiazhuang, Hebei, 050091, China

Submission Info

Communicated by Z. Sabir
Received June 22, 2022
Accepted November 11, 2022
Available online May 16, 2023

Abstract

Due to the diversified development trend of modern architectural design, the functional design and application of houses are being presented in the interior space color layout of houses with its many advantages of interactivity, comprehensiveness, multi-functionality, and personalization. With this as the starting point, this paper analyzes the psychological perception of survey respondents on the same spatial color through big data, converts the perception into EEG signal for decoding, and after the decoding process of EEG data pre-processing, feature extraction, feature identification, and classification, calculates the significance of each element in the time-frequency matrix, which can get a homo-dimensional mask matrix. Then the conditional random field model is established on the random field theory to get the parameters of the model. Finally, the parameters of the model are obtained by maximizing the following entropy function, which is brought into the Lagrangian operator to obtain the pairwise Lagrangian operator. Finally, the EEG signal is decoded to realize the self-control training of color perception under different mentalities. The experimental results showed that by performing the intervention test on self-control and color insight, the mean value of the total self-control score in training was 61.99±11.45, and the intervention effect had stability. Therefore, improving self-control ability and forming correct tendency psychological perception plays a vital role in the color design of architectural space.

Keywords: Modern architectural design; Interior space color; Psychological perception; EEG signal; Color insight
AMS 2020 codes: 91E30

†Corresponding author.
Email address: fengwei19881020@163.com

ISSN 2444-8656
https://doi.org/10.2478/amns.2023.1.00259

1 Introduction

In interior space decoration design, interior architectural color decoration is of great significance, and with the visual beauty and psychological implication of color itself, it can build interior space design with different themes and different atmospheres through artistic and humanistic architectural color combinations [1-3]. In terms of the function of architectural color itself, different architectural colors can produce different visual impressions and psychological responses, for example, red can stimulate the psychological excitement of the nervous system and make the human body feel energetic and passionate [4-5]. Therefore, red is often used in wedding rooms, sports spaces, etc., and then blue can lower the pulse rate and create a quiet and comfortable space atmosphere, which is often used in bedroom decoration and resting places; in terms of the function of architectural color combinations, different architectural colors can produce different visual illusions, for example, the color matching method of light ceiling color and dark ground color is used in interior space decoration, which can increase people's For example, the use of the color combination of light ceiling color and dark ground color in interior space decoration can increase the sense of interior space hierarchy and make the interior space feel larger [6]. The reasonable use of architectural color and optical illusion can build a new, interactive, and interesting new interior space through the artistic matching of interior space color, breaking the fetters of traditional interior space decoration design thinking. Therefore, the design interaction between architectural color and optical illusion should be strengthened and gradually applied to the interior space decoration. Architectural color has a regulating and beautifying effect on the interior space atmosphere decoration for optical illusion [7]. For example, architectural color detailing can reconceptualize a space by adding white and gray tones to create a clean, quiet interior. The top space decoration is the finishing touch to the overall design, and the sky pattern with green and blue colors can add a natural and green atmosphere to the interior space environment, and visually give people the illusion of being under white clouds [8-13]. The psychological community calls this thinking "theoretical psychology," which is roughly equivalent to philosophical thinking about a wide range of psychological content. The current psychological community lacks an effective supply of psychological knowledge, especially theoretical knowledge at the meso and macro levels. As scientific research progresses, researchers should focus on training their underlying logical thinking so that they are bold enough to "disprove" old theories and create new ones [14-16]. The development of psychology cannot, in any way, escape from the underlying framework of humanistic philosophical thinking about the practice of "subjectivity" in history and culture. As we all know, color has a sense of weight and movement, and can create spatial biases in human perception. The eye is an important organ of our body, and vision is an important way to capture information about our environment [17]. Studies have shown that the central and peripheral vision form the structure of the human retina and that the visual functions of the central and peripheral vision are different. Most of the environmental information received by the human brain is captured visually, and the impact of color on vision is the greatest and most intuitive. Different colors may bring different feelings to people, and colors that make people feel warm, comfortable, and cheerful are warm, while colors that make people feel calm or even cold are cold [18-21]. In color, red and yellow are warm colors, which can bring people a warm psychological experience and can stimulate people's visual nerves and improve their activity; green and blue are cool colors, which can bring people a cold and quiet psychological experience and make them feel cool; in architectural design, a bright and warm environment can make people feel happy and promote brain cell development, while on the contrary, in a dark and cold On the contrary, in a dark and cold environment, people are more likely to have a depressed mood, which is not conducive to healthy physical and mental growth. In the visual warm color will be more prominent, so people in the surrounding environment will first see the warm color, in the space, it will produce the illusion of reduced distance, the visual cold color will be relatively backward, in the space people tend to feel the illusion of increased distance. In the architectural space, cold and warm with the whole space can make a stronger sense of space, can effectively beautify the

architectural environment. Two colors with the same area, high brightness, and light color have the effect of enlargement, while low brightness and dark color have the effect of reduction [22]. This is also the case with the design details of housing architecture, where bright-colored decorations appear thicker and darker ones appear smaller.

The spatial design of architecture cannot be separated from the development of psychology, and researchers in spatial psychology always remind themselves that the first psychology laboratory founded by Vonte at the University of Leipzig in 1879 was the day when spatial psychology "broke out of its cocoon", but its real integration into the field of color design has a hidden and complex historical opportunity [23]. In the 1920s, the fledgling psychology ran head-on into the hegemony of logical empiricism. As a result, psychologists as a whole were more receptive to empiricist ideas than most of their counterparts in other social sciences. The pace of empiricization among European psychologists was slowed by their traditional tendency toward continental rationalism [24-25]. However, historical and geographical trends coupled to produce an unprecedented surge of empiricist sentiment in North America in the early to mid-20th century. Arguably, no group of scholars in any discipline emphasized the empirical aspect of the pursuit of knowledge more than the radical behaviorists. This influence was passed down through two generations of behaviorist psychologists, finally culminating in the 1950s [26]. The great neo-behaviorist psychologist Skinner was its most influential spokesperson, who argued that there are no theoretical problems in science. According to Skinner, even logical problems should be solved by doing experiments. In the behaviorist psychologist's understanding of quantitative science, "theory" (theory) is considered secondarily, if not completely, aside. If there was any role for theory in psychological research, it came into play only after quantitative research had uncovered the laws of psychological reality, and Skinner even admitted after decades of behavioral research that radical behavioral theories had still not emerged. Without some kind of conceptual framework, individual observations remain largely isolated and their meaning is often mysterious, if not useless [27-29]. It is the cumulative and general impact of a body of knowledge, rather than the specificity of individual findings, that leads to prediction and control and all other advances from scientific inquiry. While individual experiments may inspire, stimulate, and illuminate the dark corners of once ignorance, they are meaningless until their meaning is clear. Just as flames are fascinating and beautiful in color perception, when the principles behind the dazzling glow emitted by flames during combustion are revealed, deeper insights and theories become possible, and science crosses from mystery to comprehensibility. Similarly, the color design of architecture is not isolated; it is inextricably linked to the heart of the observer.

Therefore, in this paper, by decoding the EEG signal, through the decoding process of EEG data pre-processing, feature extraction, feature identification, and classification, an iso-dimensional mask matrix is obtained by calculating the significance of each element in the time-frequency matrix. Then the conditional random field model is established on the random field theory to get the parameters of the model. Finally, the parameters of the model are obtained by maximizing the following entropy function, which is brought into the Lagrangian operator to obtain the pairwise Lagrangian operator. This is used as a basis to realize the self-control training of spatial color design under different states of mind. The emergence of psychology makes architectural design training more diverse, cutting-edge, and efficient. For color design that closely combines theory and practice, the application of psychology can not only broaden the breadth and width of color design, but also show every aspect of the design process accurately, carefully, and vividly in the final architectural space, and can enhance the cross-influence of psychology and spatial color design.

2 Spatial color design based on environmental psychology

2.1 Decoding algorithm of EEG signal

The decoding process of EEG signals can be mainly divided into three steps: EEG data pre-processing, feature extraction, feature identification, and classification. In this paper, by introducing the EEG signal decoding algorithm to the new media environment, the self-control training method of vocal performance teaching is calculated and the boundary decision parameter algorithm based on the time-frequency mask method is proposed. the EEG signal decoding process is shown in Figure 1.

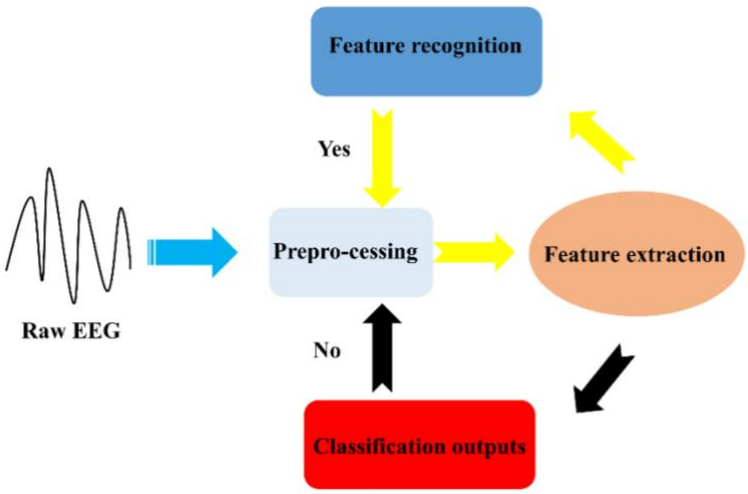

Figure 1. EEG signal decoding process

The pre-processing algorithms mainly include temporal filtering such as low-pass filtering, band-pass filtering, Kalman filtering, RobustKalman filtering, nonlinear filtering, etc.; spatial filtering such as common mean reference, Laplacian reference, etc.; and algorithms such as principal component analysis, blind source separation, reference independent component analysis, etc. Feature extraction algorithms mainly include: Fourier transform, adaptive regression model, wavelet transform, independent component analysis, common spatial pattern, common spatial-spectral filtering, phase synchronization feature analysis, etc. The pattern classification algorithms mainly include decision trees, linear discriminant analysis, Bayesian classifiers, neural networks, support vector machines, etc.

2.2 Time-frequency masking method

The time-frequency mask method can calculate the significance of the spectral energy difference of each time-frequency point under different tasks, and search for the relatively most different feature points eeg time series data are transformed into a time-frequency representation of data by short-time Fourier transform STFT). For each lead, their time-frequency distribution matrix is obtained in the same way. The time-frequency distribution matrix is expressed as follows.

$$P(f,t)=\begin{bmatrix} p_{f_1t_1} & p_{f_2t_2} & \cdots & p_{f_1t_n} \\ p_{f_2t_1} & p_{f_2t_2} & \cdots & p_{f_2t_n} \\ \vdots & \vdots & \ddots & \vdots \\ p_{f_mt_1} & p_{f_mt_2} & \cdots & p_{f_mt_n} \end{bmatrix} \tag{1}$$

Where the frequency grows from f_1 to f_m with the rows and the time grows from t_1 to t_n with the columns, so each element of the matrix is the energy at the frequency f_i and moment point t_j. To reduce the computational effort, the sub-time-frequency distribution matrix can be selected according to the actual research problem as follows.

$$P^s(f,t)=\begin{bmatrix} p^s_{f_1t_1} & p^s_{f_1t_2} & \cdots & p^s_{f_1t_n} \\ p^s_{f_2t_1} & p^s_{f_2t_2} & \cdots & p^s_{f_2t_n} \\ \vdots & \vdots & \ddots & \vdots \\ p^s_{f_mt_1} & p^s_{f_mt_2} & \cdots & p^s_{f_mt_n} \end{bmatrix} \tag{2}$$

Then the t-test is used to measure the significance of the difference between each element of the time-frequency matrix under the two categories and find the element with higher significance. By calculating the significance of each element in the time-frequency matrix, we can obtain an iso-dimensional mask matrix.

$$M^s(f,t)=\begin{bmatrix} M^s_{f_1t_1} & M^s_{f_1t_2} & \cdots & M^s_{f_1t_n} \\ M^s_{f_2t_1} & M^s_{f_2t_2} & \cdots & M^s_{f_2t_n} \\ \vdots & \vdots & \ddots & \vdots \\ M^s_{f_mt_1} & M^s_{f_mt_2} & \cdots & M^s_{f_mt_n} \end{bmatrix} \tag{3}$$

In this mask matrix, the positions of elements with significance in the corresponding time-frequency matrix are set to 1, and other positions without significance are set to 0. Considering that the difference of energy has positive and negative values, two mask matrices are constructed, positive mask matrix M_P and negative mask matrix M_N, respectively. Finally, after calculating the average of the elements left after point multiplication of the positive and negative mask matrix by the time-frequency matrix, respectively, two features can be obtained for each lead.

$$f_P=\frac{1}{N_P}\sum_{f=f_1}^{f_m}\sum_{t=t_1}^{t_n}M_P^s(f,t)P^s(f,t) \tag{4}$$

$$f_N=\frac{1}{N_N}\sum_{f=f_1}^{f_m}\sum_{t=t_1}^{t_n}M_N^s(f,t)P^s(f,t) \tag{5}$$

Where N_P and N_N are the number of elements of the positive and negative mask matrices M_P and M_N of the neutralization, respectively. Repeating the above process for each lead, two features can be obtained, and the features of all leads form a feature vector as follows

$$V_{Power}=\left[f_P^1 f_P^2 \ldots f_P^n f_N^1 f_N^2 \ldots f_N^n\right]^T \tag{6}$$

Where n is the number of leads used for feature extraction.

The conditional random field (CRF) model is built on the random field theory, $G=(V,E)$ and the sequence $Y=(Y_v)_{v\in V}$ of random variables on the set of vertices of G. For a sequence X of random variables, if the relationship between X and Y satisfies the following Markov property, i.e.

$$P\left(Y_\upsilon \middle| X, Y_\omega, \omega\neq\upsilon\right)=P\left(Y_\upsilon \middle| X, Y_\omega, \omega \quad \upsilon\right) \tag{7}$$

Where ω is adjacent to v in the graph $G,(X,Y)$, is said to be a conditional random field.

From the above definition, it can be seen that the conditional random field model satisfies the definition of a Markov random field. Assuming that the set of variables of the Markov random field is $S = (y_1, y_2, \cdots, y_n)$, we can define:

$$P(y_1, y_2, ..., y_n) = \frac{1}{Z} * \exp^{-\frac{1}{T} * U(y_1, y_2, ..., y_n)} \tag{8}$$

Where Z is the normalization factor that is used to ensure that this probability satisfies the fundamental axiom $U(y_1, y_2, \cdots, y_n)\ T$ of probability generally known as the energy function. In the Markov random field corresponding to the signal, each cluster in the signal (complete signal) corresponds to a function, and this joint probability form is also called Gibbs distribution, i.e., as

$$G = \left(V = 1, 2, , m, E = (i, i+1)\right) \tag{9}$$

Thus, the conditional random field is defined under the single-chain graph model, given a sequence X of conditions, the conditional distribution of the sequence Y as the following form.

$$P_\theta\left(Y \middle| X\right) \infty \exp\left(\sum_{e \in E, k} \lambda_k f_k\left(e, Y\middle|_e, X\right) + \sum_{\upsilon \in V, k} \mu_k g_k\left(\upsilon, Y\middle|_\upsilon, X\right)\right) \tag{10}$$

Here, $Y|_s$ represents the part of the sequence Y of nodes associated with the sub-signal S of the graph G.

$\theta = \{\lambda_1, \lambda_2, \lambda_3, \ldots, \lambda_m, \mu_1, \mu_2, \mu_3, \ldots, \mu_n\}$ represents the corresponding parameter of the model. The function f_k and g_k can be considered as a fixed feature function. Thus, the problem is now to learn the parameters of the model from the training data $D = \{x^i, y^i\}_{i=1}^N$.

To simplify the training of the parameters, it is straightforward to define the parameter matrix W of the model. Thus, it is possible to change the conditional distribution of the sequence Y^i for a given sequence X^i case from Equation 2.8 to

$$P_W\left(Y^i \middle| X^i\right) \infty \exp\left(\sum W * X^i\right) \tag{11}$$

For obtaining the parameters of the model, the maximum entropy principle can be used to solve it. Thus, the parameters of the model can be obtained by maximizing the following entropy function.

$$Opt(W) = \sum_{i=1}^{N} \log P_W\left(Y^i \middle| X^i\right) \tag{12}$$

$$\infty \sum_{X,Y} \tilde{P}_D\left(X, Y\right) \log P_W\left(Y \middle| X\right) \tag{13}$$

$$\infty \sum_{X,Y} \tilde{P}_D\left(X, Y\right) \sum W * X \tag{14}$$

The parameter matrix W defines the conditional distribution density of the data features and determines the distribution of different classes of EEG data in space.

A two-class classification problem with N training samples is used as an example. Each sample is represented as a binary group $(x_i, y_i)(i = 1,2,\cdots,N)$, where $x_i = (x_{i1}, x_{i2}, \ldots, x_{id})^T$, corresponds to the attribute set of the ith classification sample. Let $y_i \in \{-1,1\}$ denote his category label. The decision boundary of a linear classifier can be expressed by the following equation.

$$w \cdot x + b = 0 \tag{15}$$

Where W and b are the model parameters.

For training sample sets where singularities exist, it is necessary to utilize a method called soft edges. This can be achieved by introducing positive-valued slack variables in the optimization problem constraint.

$$\begin{cases} w \cdot x_i + b \geq +1 - \xi_i & if \quad y_i = +1 \\ w \cdot x_i + b \leq -1 + \xi_i & if \quad y_i = -1 \end{cases} \tag{16}$$

Where $\forall i: \xi_i > 0$ rewrites the objective function as

$$f(w) = \frac{\|w\|^2}{2} + C(\sum_{i=1}^{N} \xi_i)^k \tag{17}$$

Where the parameters C and k regulate the penalty on the misclassified training samples. To simplify the problem, assume that the values are chosen to be fixed $k = 1$. The parameter C can be obtained based on the classification performance of the samples on the optimal training set. The Lagrangian operator of the constrained optimization problem can be modified as

$$L_p = \frac{1}{2}\|w\|^2 + C\sum_{i=1}^{N} \xi_i - \sum_{i=1}^{N} \lambda_i \left\{ y_i \left(w \cdot x_i + b \right) - 1 + \xi_i \right\} - \sum_{i=1}^{N} \mu_i \xi_i \tag{18}$$

The inequality constraint can be transformed into an equation constraint using the following KKT condition.

$$\xi_i \geq 0, \lambda_i \geq 0, \mu_i \geq 0 \tag{19}$$

$$\lambda_i \left\{ y_i \left(w \cdot x_i + b \right) - 1 + \xi_i \right\} = 0 \tag{20}$$

$$\mu_i \xi_i = 0 \tag{21}$$

Let the first-order derivatives of L_p with respect to w, b and ξ_i be zero, we have

$$\frac{\partial L_p}{\partial \xi_i} = C - \lambda_i - \mu_i = 0 \Rightarrow \lambda_i + \mu_i = C \tag{22}$$

Taking into the Lagrangian operator, the following dual Lagrangian operator is obtained.

$$\begin{aligned} L_D &= \frac{1}{2}\sum_{i,j}\lambda_i\lambda_j y_i y_j x_i \cdot x_j + C\sum_i \xi_i - \sum_i \lambda_i \left\{ y_i \left(\sum_j \lambda_j y_j x_i \cdot x_j + b \right) - 1 + \xi_i \right\} \\ &\quad - \sum_i (C - \lambda_i)\xi_i \\ &= \sum_{i=1}^{N} \lambda_i - \sum_{i,j} \frac{1}{2} \lambda_i \lambda_j y_i y_j x_i \cdot x_j \end{aligned} \tag{23}$$

It is the same as the dual Lagrangian operator on linearly separable data. Similarly, the multipliers can be brought into the formula and the KKT condition to obtain the boundary decision parameters. Through the above calculations, color design in architectural space based on environmental psychology can be realized. The architectural structure and the color inside the space are closely linked and inseparably unified with the mental activity of the occupants. Often a person's heart thoughts will have a great impact on the color perception of the building.

3 Experimental design and discussion of experimental results

The experimental design model used in this study is: two experimental groups and a blank control group, trying to test the effect of different psychological object space color perception situations through the experimental results of different groups and to explore which scheme is more effective.

Experimental group A was only trained in self-control, and experimental group B was simultaneously trained in self-control and spatial insight intervention. To prevent the inaccuracy of the results caused by the subjects' growth and development, a blank control group was set up without intervention, and the basic model of the specific experimental design is shown in Table 1.

Table 1. Basic model of experimental design

	Experimental group A	Experimental group B	Blank control group
Pre-test	A1	B1	C1
Experimental treatment	Self-control	Vocal performance insight + self-control	Without any training
post test	A2	B2	C2
Delayed test	A3	B3	C3

First, the study was conducted with young people in the society who are choosing to purchase a house as the research subjects. 400 questionnaires were distributed, and 366 valid questionnaires were finally collected, with an effective rate of 96%. Among the 366 valid questionnaires, subjects who were eligible and willing to participate in group counseling activities were screened and contacted. 60 subjects were finally identified under various conditions such as time constraints, and the number of subjects included in the experimental group A, group B, and the blank control group were 20, 21, and 19 respectively after random assignment of the subjects.

Intervention: Group A was given group coaching on self-control training once a week for 6 times, with an average of 90-120 minutes each time; Group B was given group coaching on insight as well as self-control training once a week 6 times, with an average of 90-120 minutes each time; the control group was not given any training.

To ensure that the time spent in group counseling was the same for Experiment A and Experiment B, the self-control training activities included in Group A were conducted more slowly than those in Group B in each unit of group counseling. At the end of the group counseling, the questionnaire used in the pre-test was administered uniformly to the 60 subjects, and the members' spatial insight of the

house and self-control was measured again. Two months after the end of the group counseling, the questionnaire was administered to all subjects for a delayed posttest to examine the stability of the intervention effect. Then, the data of insight and self-control were statistically analyzed, and the results calculated by the decoding algorithm of EEG signals are shown in Table 2.

Table 2. Current status of spatial insight and self-control

	M	SD	Average score per question	Highest score	Lowest Score
Vocal Performance Insight	85.78	11.52	3.63	106	61
Self-control	61.99	11.45	3.31	97	25

Table 2 shows that the mean spatial insight score is 85.78±11.52, and the overall score is moderate to high, which is the same as the results of previous studies, using the median "3" of the scale as the degree division. Their mean control score was 61.99±11.45, with an overall score slightly above the median, which is the same as the findings obtained in previous studies.

To ensure that the method of testing the results of group counseling was correct and valid, an ANOVA was conducted on the pretest scores of the two groups before group counseling to examine whether the subjects were homogeneous in terms of variables.

Table 3. Homogeneity test of the two groups of subjects

	Experimental group A		Experimental group B		Blank control group		
	M	SD	M	SD	M	SD	F
Vocal performance insight	74.45	9.02	77.02	6.23	74.02	7.96	1.458
Self-control	50.34	10.74	52.12	8.78	50.76	8.44	0.215

It can be concluded that: in the pre-test, the two groups of subjects did not differ significantly in their scores on the variables, which means that the two groups of subjects were homogeneous in the pre-test and met the requirements of the balanced group experimental design. In the subsequent data statistics, repeated measures ANOVA can be used to test the differences between and within groups and thus conclude the experiment.

A posttest was administered to both groups of subjects immediately after the last actual house observation, and the delayed posttest was completed two months later. After the total scores of insight were obtained, a 3x3 repeated measures ANOVA was conducted to analyze whether there were differences in the total scores of experimental groups A and B and the control group at the three time points, with test time (pre-test, post-test, and delayed post-test) as the within-subject variable and group (experimental groups A and B, control group) as the between-subject variable, and the results showed that the interaction between test time and the group was significant, the main effect of time was significant, and the main effect of the group The significant main effects of time and group are shown in Figure 2.

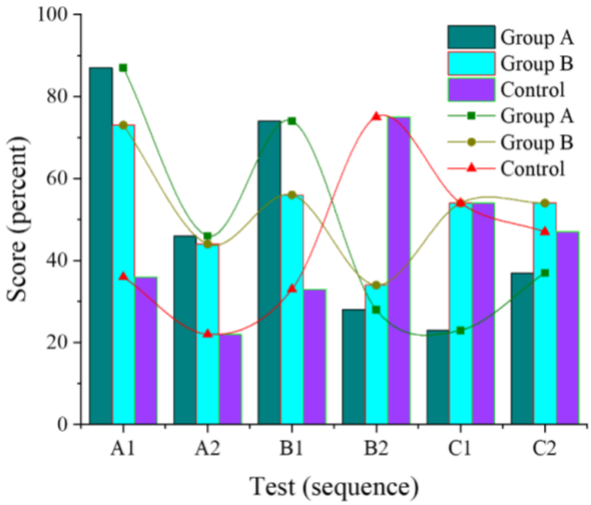

Figure 2. Interaction between measurement time and group on insight

From the simple effect analysis in Figure 2, it was found that in the pre-test of insight, there was no significant difference between the three groups after the Lagrangian arithmetic calculation. In the post-test, there was a significant difference between the three groups. In the delayed posttest, there were significant differences among the three groups. The insight of group A and the control group without relevant content intervention did not change significantly, and the insight scores of subjects in both groups were significantly lower than those in group B. The intervention program in group B was effective in improving subjects' future time insight, and the effect remained stable and stable two months after the intervention.

To analyze whether the total scores of experimental groups A, B, and the control group differed at the three-time points, a 3x3 repeated measures ANOVA was conducted with insight as a within-subjects variable and different groups as between-subjects variables, and the results showed that the test group and time effects were significant, the main effect of time was significant, and the main effect of time significantly interacted as shown in Figure 3.

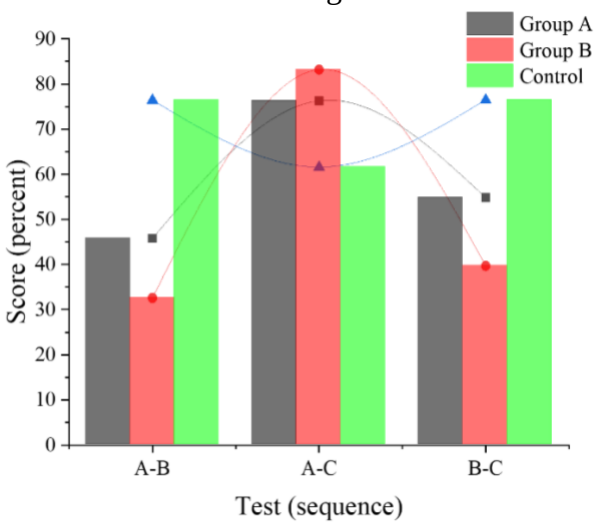

Figure 3. Interaction between measurement time and group on self-control

From the simple effect analysis in Figure 3, it was found that in the self-control pre-test, there was no significant difference between the three groups after the Lagrangian operator calculation. In the self-control post-test, there was a significant difference between the three groups. In the self-control delayed posttest, there was a significant difference between the three groups. Both groups scored

significantly higher on the self-control delayed posttest than the control group. The two group counseling programs were effective and stable in improving self-control compared to the blank control group. From the measurements of groups A and B, the subjects in both groups experienced a significant increase in self-control after the intervention, indicating that the manipulation of another independent variable, self-control, was effective and increased with the gradual increase in resources. The learning of self-control strategies allows individuals to identify the situations in which they are prone to problem behaviors so that they learn to use different methods to better manage and reinforce self-control behaviors and take the opportunity to achieve individual growth.

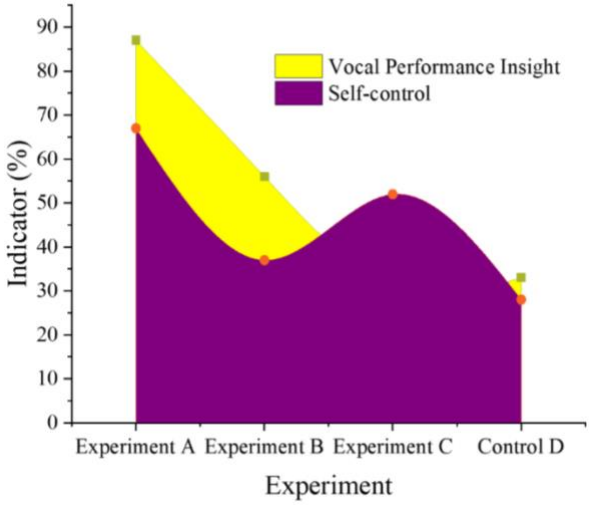

Figure 4. The Role of Insight and self-control training

From the analysis of Figure 4, it is easy to see that in the insight-related test, there is no significant difference between the four groups after the Lagrange arithmetic calculation. In the self-control post-test, there is a significant difference between A and B. In the delayed self-control post-test, there was a significant difference between the four groups. The scores of the delayed self-control post-test were significantly higher in groups B and C than in the control group. The two group counseling programs were effective and stable in improving self-control compared to the blank control group. From the measurement results of groups A and B, a significant increase in self-control occurred in both groups of subjects after the intervention, indicating that self-control diminished as the number of observed house types gradually increased.

4 Conclusion

With the rapid development and popularity of psychology, how to innovatively use the "new media" technology to optimize and improve the traditional spatial color judging mode is the key factor to enriching the evaluation standard and mode promotion under the role of psychology in different environments. As an important part of the architectural evaluation process, spatial color plays a very active role in the self-control and observation reading of the evaluator. In this study, the intervention training of investigators from the perspective of self-control and spatial color insight, the following conclusions were drawn.

1) The mean value of the total self-control score in the self-control training was 61.99 ± 11.45, with an overall score slightly above the median, and the intervention effect was stable. A significant increase in self-control occurred after the intervention, and the scores were still higher in the delayed test than in the previous test.

2) The mean value of the total color insight score was 85.78±11.52, and the insight was at a moderate to a high level. The method that simultaneously improved color insight and self-control had higher values than the method that only improved self-control.

References

[1] Larose, R., Gregg, J. L., Strover, S., et al. (2015). Closing the rural broadband gap: Promoting adoption of the Internet in rural America. Telecommunications Policy, 31(6-7), 359-373.

[2] Baltes, S., Park, G., & Serebrenik, A. (2020). Is 40 the new 60? How popular media portrays the employability of older software developers. IEEE Software, PP(99).

[3] Yao, S., Zhao, Y., Zhang, A., et al. (2018). Deep Learning for the Internet of Things. Computer, 51(5), 32-41.

[4] Ramezani, P., & Jamalipour, A. (2017). Toward the Evolution of Wireless Powered Communication Networks for the Future Internet of Things. IEEE Network.

[5] D Y, Takahashi, A R. (2015). LANGUAGE DEVELOPMENT. The developmental dynamics of marmoset monkey vocal production. Science (New York, N.Y.).

[6] Lingala, S. G., Zhu, Y., Kim, Y. C., et al. (2017). A fast and flexible MRI system for the study of dynamic vocal tract shaping. Magnetic Resonance in Medicine, n/a-n/a.

[7] Peng, L., & Tao, G. (2017). Acoustical characteristics of Chinese musical instrument bamboo flute. The Journal of the Acoustical Society of America, 141(5), 3726-3726.

[8] Lawless, M. S., Baglione, M., & Sidebotham, G. W. (2016). Developing and teaching an interdisciplinary musical instrument design course at the Cooper Union. Journal of the Acoustical Society of America, 139(4), 2096-2096.

[9] Saitis, C., & Kai, S. (2020). Brightness perception for musical instrument sounds: Relation to timbre dissimilarity and source-cause categories. The Journal of the Acoustical Society of America, 148(4), 2256-2266.

[10] Kusumaningtyas, I., Christianto, R., & Parikesit, G. O. (2020). Directivity of the half-dome bundengan musical instrument. The Journal of the Acoustical Society of America, 148(4), 2749-2749.

[11] Jiang, X., & Pell, M. D. (2015). On how the brain decodes vocal cues about speaker confidence. Cortex, 66, 9-34.

[12] Rollins, M. K., Berardi, M. L., Hunter, E. J., et al. (2015). Vocal fatigue over a workday: A schoolteacher case study. Journal of the Acoustical Society of America, 137(4), 2434-2434.

[13] Zhang, Z. (2019). Estimation of vocal fold geometry and stiffness from voice acoustics. The Journal of the Acoustical Society of America, 146(4), 3085-3086.

[14] Kaburagi, T., & Fukuda, Y. (2017). Observation of the vocal tract configuration while playing a woodwind instrument. The Journal of the Acoustical Society of America, 141(5), 3875-3875.

[15] Bda, B., Rs, A., & Nk, A. (2020). Processing communicative facial and vocal cues in the superior temporal sulcus. NeuroImage, 221.

[16] Engesser, S., Crane, J., Savage, J. L., et al. (2015). Experimental Evidence for Phonemic Contrasts in a Nonhuman Vocal System. PLoS Biology, 13(6), e1002171.

[17] Astolfi, A. (2018). Trajectories in classroom acoustics: The vocal behaviour of teachers. The Journal of the Acoustical Society of America, 144(3), 1977-1977.

[18] Arnela, M., & Guasch, O. (2017). Finite element simulation of diphthongs in three-dimensional realistic vocal tracts with flexible walls. Journal of the Acoustical Society of America, 141(5), 3469-3469.

[19] Acheson, N. H. (2021). Multiple sub-repertoires and singing patterns of Red-eyed Vireos (Vireo olivaceus). The Wilson Journal of Ornithology, 132(3).

[20] Dai, J., & Dixon, S. (2019). Singing together: Pitch accuracy and interaction in unaccompanied unison and duet singing. Journal of the Acoustical Society of America, 145(2), 663-675.

[21] Rachel, M., Bittner, et al. (2019). An Introduction to Signal Processing for Singing-Voice Analysis: High Notes in the Effort to Automate the Understanding of Vocals in Music. IEEE Signal Processing Magazine, 36(1), 82-94.

[22] C J, Mortensen, A M, et al. (2015). The flipped classroom stimulates greater learning and is a modern 21st-century approach to teaching today's undergraduates. Journal of animal science.

[23] Farshchin, M., Camp, C. V., & Maniat, M. (2016). Multi-class teaching-learning-based optimization for truss design with frequency constraints. Engineering Structures, 106, 355-369.

[24] Barve, S., Taylor, C., & Viral, J. (2017). Jack of All Calls and Master of Few: Vocal Mimicry in the Tawny Lark (Galerida Deva). Avian Biology Research, 10(3), 174-180.

[25] Nix, J. P. (2015). Listener preferences for vibrato rate and extent in synthesized vocal samples. Journal of the Acoustical Society of America, 137(4), 2404-2405.

[26] Nort, D. V. (2018). Audio-haptic perception in immersive improvisational environments. The Journal of the Acoustical Society of America, 143(3), 1931-1931.

[27] Lemaitre, G., Jabbari, A., Misdariis, N., et al. (2016). Vocal imitation of basic auditory features. The Journal of the Acoustical Society of America, 139(1), 290-300.

[28] Hara, E., Perez, J. M., Whitney, O., et al. (2015). Neural FoxP2 and FoxP1 expression in the budgerigar, an avian species with adult vocal learning. Behavioural Brain Research, 283, 22-29.

[29] Carey, D., & McGettigan, C. (2017). Magnetic resonance imaging of the brain and vocal tract: Applications to the study of speech production and language learning. Neuropsychologia.